PERFORMANCE OF MULTI-HARMONIC RF FEEDFORWARD SYSTEM FOR BEAM LOADING COMPENSATION IN THE J-PARC RCS

Fumihiko Tamura*, Masanobu Yamamoto, Chihiro Ohmori, Alexander Schnase, Masahito Yoshii, Masahiro Nomura, Makoto Toda, Taihei Shimada, Keigo Hara, Katsushi Hasegawa
J-PARC Center, KEK & JAEA, Tokai-mura, Naka-gun, Ibaraki-ken, Japan 319-1195

Abstract

The beam loading compensation is a key part for acceleration of high intensity proton beams in the J-PARC RCS. In the wide-band MA-loaded RF cavity, the wake voltage consists of not only the accelerating harmonic component but also the higher harmonics. The higher harmonic components cause the RF bucket distortion. We employ the RF feedforward method to compensate the multi-harmonic beam loading. The full-digital feedforward system is developed, which compensates the first three harmonic components of the beam loading. We present the results of the beam test with a high intensity proton beam (2.5×10^{13} ppp). The impedance seen by the beam is greatly reduced, the impedance of the fundamental accelerating harmonic is reduced to less than 25 Ω in a full accelerating cycle, while the shunt resistance of the cavity is in the order of 800 Ω. The performance of the feedforward system is promising for achievement of the design beam power, 1 MW, in the future.

INTRODUCTION

The 3 GeV rapid cycling synchrotron (RCS) of the Japan Proton Accelerator Research Complex has been commissioned aiming at 1 MW output beam power at design. The parameters of the RCS and its RF system are listed in Table 1. We have demonstrated successful acceleration of 3.3×10^{13} ppp in single-shot operation, which is equivalent to 400 kW beam power at 25 Hz operation.

We employ the magnetic-alloy (MA) cavities to generate high accelerating voltages, 400 kV per turn at the maximum with 11 cavities. The wide-band ($Q = 2$) frequency response covers the accelerating frequency sweeps, and the dual-harmonic operation, in which each cavity is driven by the superposition of the fundamental accelerating RF ($h = 2$) and the second harmonic ($h = 4$). The dual-harmonic operation enables the bunch shape control for alleviating the space-charge effects [1].

On the other hand, the wake voltage in the cavities consists of not only the accelerating component but also the higher harmonics, which cause the RF bucket distortion. For acceleration of high intensity beams, the beam loading compensation must be multi-harmonic. Therefore, we developed a multi-harmonic RF feedforward system, for the most important three harmonics ($h = 2, 4, 6$) [2].

The block diagram of the feedforward system is shown in Fig. 1. The I/Q detection technique is used to pick up the I/Q vectors for the selected harmonics. The vectors are distributed to the modules for 12 cavities and the compensation RF signals are generated by I/Q modulation with the gain and phase patterns. The compensation signals of the harmonics are summed up. The feedforward output signal is sent to the summation amplifier and the cavity is driven by a superposition of the driving RF and the feedforward compensation signal. The commissioning of the feedforward is the adjustment of the gain and phase patterns, so that the compensation signal cancels the wake voltage in the cavity.

Table 1: Parameters of the J-PARC RCS and its RF systems

circumference	348.333 m
energy	(design) 0.400–3 GeV
	(present) 0.181–3 GeV
beam intensity	(design) 8.3×10^{13} ppp
	(achieved) 3.3×10^{13} ppp
accelerating frequency	0.938–1.671 MHz
harmonic number	2
maximum rf voltage	(design) 450 kV
	(achieved) 400 kV
repetition	25 Hz
No. of cavities	(design) 12
	(installed) 11
Q-value of rf cavity	2

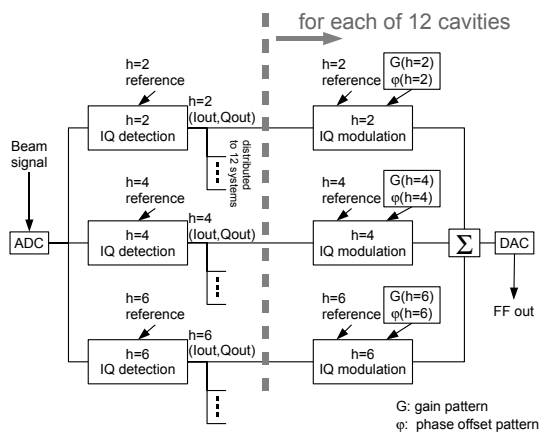

Figure 1: Block diagram of the multi-harmonic feedforward system.

* fumihiko.tamura@j-parc.jp

Copyright © 2011 by IPAC'11/EPS-AG — cc Creative Commons Attribution 3.0 (CC BY 3.0)

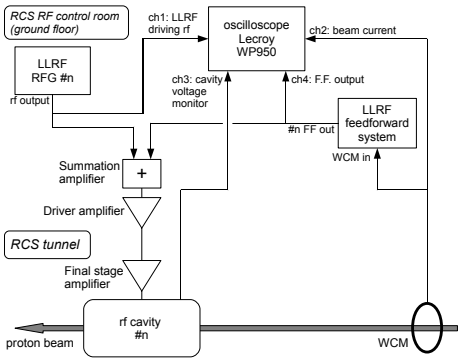

Figure 2: Feedforward commissioning setup. #n is the cavity number.

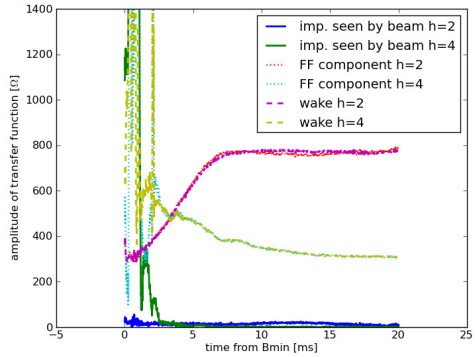

Figure 3: Comparison of the feedforward transfer function and the impedance seen by the beam.

COMMISSIONING OF MULTI-HARMONIC FEEDFORWARD

The commissioning setup is shown in Fig. 2. The commissioning of the feedforward is performed for each cavity. The following signals are recorded by the long memory oscilloscope: (i) LLRF driving rf (ch. 1); (ii) WCM signal (ch. 2); (iii) cavity gap voltage monitor (ch. 3); (iv) feedforward output (ch. 4). The sampling rate is 200 Ms/s and 4.15 M points are more than sufficient to cover the full accelerating period (20 ms). The harmonic analysis is performed on the PC and the complex amplitudes of the harmonics ($h = 2, 4, 6$) are obtained. The beam commissioning was performed with a high intensity beam, 2.5×10^{13} ppp. We established a commissioning methodology of the feedforward. For the important two harmonics ($h = 2, 4$), the following procedure is performed.

First, we obtain the transfer function from the driving rf to the cavity voltage (Step 1). The harmonic analysis is performed on the full waveform of the LLRF driving RF signal and the cavity voltage monitor without accelerating the beam. The transfer function ($H_{\rm dr}^{\rm cav}(h,t)$) is obtained as

$$H_{\rm dr}^{\rm cav}(h,t) = \frac{V_{\rm cav}(h,t)}{V_{\rm dr}(h,t)}, \qquad (1)$$

where $V_{\rm dr}(h,t)$ and $V_{\rm cav}(h,t)$ are the complex amplitudes of the LLRF driving RF and cavity voltage, respectively.

For the second harmonic ($h = 4$), the program voltage becomes zero during acceleration. To avoid the errors due to small denominators, we set $H_{\rm dr}^{\rm cav}(h,t) = 0$ when $V_{\rm dr}(h,t)$ is smaller than a certain small threshold.

Next, we obtain the impedance seen by beam under the condition of the tube currents with the standard accelerating voltage patterns (Step 2). To avoid the variation of the condition, this measurement is performed without the AVC loop. We set a special pattern, which generates similar voltages without AVC to the voltages with AVC. The test beam is accelerated, and the harmonic analysis is performed on the full waveform of the LLRF driving RF, the WCM, and the cavity voltage signals. In this step, the cavity voltage is the superposition of the driving rf component ($V_{\rm cav,dr}(h,t)$) and the wake voltage ($V_{\rm cav,wake}(h,t)$), as

$$\begin{aligned} V_{\rm cav}(h,t) &= V_{\rm cav,dr}(h,t) + V_{\rm cav,wake}(h,t) \\ &= H_{\rm dr}^{\rm cav}(h,t)\cdot V_{\rm dr}(h,t) + Z'_{\rm cav}(h,t)\cdot I_{\rm beam}(h,t), \end{aligned} \qquad (2)$$

where $Z'_{\rm cav}(h,t)$ is the cavity gap impedance under the condition of the tube currents with the driving rf voltage and $I_{\rm beam}(h,t)$ is the complex component of the beam current. By using this measurement and $H_{\rm dr}^{\rm cav}(h,t)$ obtained by the step 1, we obtain the cavity gap impedance, $Z'_{\rm cav}(h,t)$.

Then, the test beam is accelerated with the AVC on and the feedforward compensation signal (Step 3). The cavity voltage is the superposition of the driving rf component, the wake voltage, and the feedforward component ($V_{\rm cav,FF}(h,t)$) as

$$\begin{aligned} &V_{\rm cav}(h,t) \\ &= V_{\rm cav,dr}(h,t) + V_{\rm cav,wake}(h,t) + V_{\rm cav,FF}(h,t) \\ &= H_{\rm dr}^{\rm cav}(h,t)\cdot V_{\rm dr}(h,t) + Z'_{\rm cav}(h,t)\cdot I_{\rm beam}(h,t) \\ &\quad + Z_{\rm FF}(h,t)\cdot I_{\rm beam}(h,t), \end{aligned} \qquad (3)$$

where $Z_{\rm FF}(h,t)$ is the transfer function from the beam current to the feedforward voltage component. By using the measured values and the impedance and transfer functions ($H_{\rm dr}^{\rm cav}(h,t)$ and $Z'_{\rm cav}(h,t)$), the transfer function $Z_{\rm FF}(h,t)$ is obtained. The impedance seen by the beam with feedforward is $Z'_{\rm cav}(h,t) + Z_{\rm FF}(h,t)$, and the pattern is modified so that the impedance is minimized. For a given beam condition, only a few iterations of the step 3 result in an impedance reduction in the order of 1/10. For fine tuning aiming to keep the impedance seen by the beam less than 25 Ω during the full accelerating period, one or two additional iterations are necessary.

The comparison of the impedance and the feedforward transfer function after the iteration of the step 3 is shown in Fig. 3. In the figure, "wake" indicates the impedance seen by the beam without feedforward, "FF component" the feedforward transfer function, and "imp. seen by the beam" is the impedance seen by the beam with the feed-

Copyright © 2011 by IPAC'11/EPS-AG — cc Creative Commons Attribution 3.0 (CC BY 3.0)

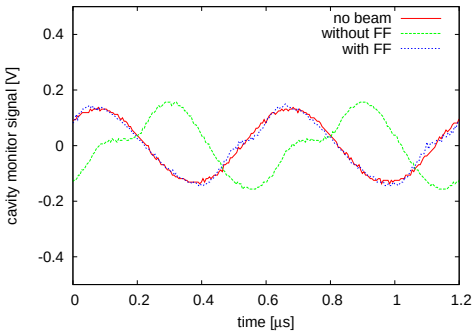

Figure 4: Comparison of cavity #1 voltage monitor waveforms with no beam, in case of acceleration of 300 kW equivalent beam without and with feedforward, just before extraction.

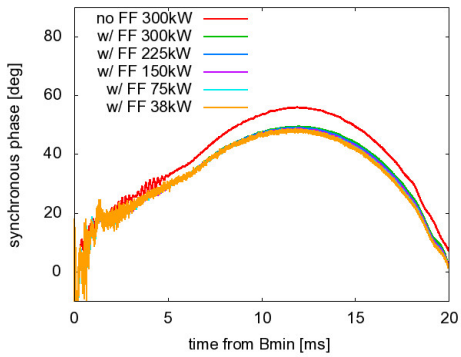

Figure 5: Comparison of ϕ_s without and with feedforward.

forward. For the fundamental harmonic ($h = 2$) the amplitude of the feedforward component is very close to the impedance seen by the beam without feedforward. The impedance seen by the beam with feedforward is less than 25 Ω during the full accelerating period, while the shunt resistance of the accelerating gap is 800 Ω. For the second harmonic, the impedance seen by the beam is less than 25 Ω after 2 ms. The feedforward system successfully reduces the impedance seen by the beam.

A comparison of the cavity voltage waveform just before extraction with no beam, with the 300 kW equivalent beam without and with feedforward is shown in Fig. 4. With feedforward, the waveform distortion by the higher harmonics is reduced. Also, the phase shift, which corresponds to the loading angle, is reduced. The waveforms with no beam and with feedforward are close.

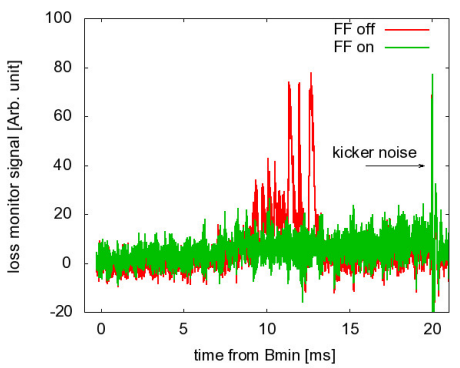

Figure 6: Beam loss monitor signals at the arc section with acceleration of the 300 kW equivalent beams.

Thus, the feedforward system works satisfactorily. For 11 cavities the feedforward patterns are adjusted, and the feedforward is used in routine operation of the RCS. Thanks to the good stability of the feedforward system itself and the high power RF system including the MA cavity, it has not been necessary to optimize the patterns again since the initial commissioining in June 2010.

REDUCTION OF THE BEAM LOSS WITH FEEDFORWARD

The distortion of the cavity voltage waveform by the higher harmonic components of the wake voltage causes a deviation of the synchronous phase (ϕ_s). This happens because the energy gain per turn at ϕ_s must be same with and without voltage distortion. In Fig. 5 the synchronous phases during an accelerating period without and with feedforward are plotted. For 300 kW equivalent beam, the maximum ϕ_s is reduced from 55 deg to 49 deg with feedforward, since the voltage waveform distortion is much smaller. Also one can see that the dependency of ϕ_s on the beam intensity is small with feedforward.

The RF buckets shrink with higher ϕ_s, which may cause beam losses at the high dispersion area in the arc sections. The beam loss monitor signals at the arc section without and with feedforward are plotted in Fig. 6. At the beam intensity of 300 kW equivalent beam, no intensity loss is observed by the DCCT, while there is a small amount of losses seen by loss monitors at the dispersion peak in the middle of the accelerating period. The losses disappear with feedforward, since the feedforward reduces the voltage distortion and ϕ_s become smaller, which keeps the margin of the RF bucket.

CONCLUSIONS

The commissioning methodology of the multi-harmonic feedforward described in this article is to be effective at the higher beam intensity. The performance of the multi-harmonic feedforward is promising for the achievement of the design beam power, 1 MW.

REFERENCES

[1] F. Tamura, et al.: "Longitudinal painting with large amplitude second harmonic rf voltages in the rapid cycling synchrotron of the Japan Proton Accelerator Research Complex", Phys. Rev. ST Accel. Beams, **12**, 041001 (2009).

[2] F. Tamura, et al.: "Multiharmonic rf feedforward system for beam loading compensation in wide-band cavities of a rapid cycling synchrotron", Phys. Rev. ST Accel. Beams, **14**, 051004 (2011).

Copyright © 2011 by IPAC'11/EPS-AG — cc Creative Commons Attribution 3.0 (CC BY 3.0)